Genuine multipartite entanglement in the cluster-Ising model

Genuine multipartite entanglement in the cluster-Ising model

S M Giampaolo and B C Hiesmayr

University of Vienna, Faculty of Physics, Boltzmanngasse 5, A-1090 Vienna, Austria
E-mail: Beatrix.Hiesmayr@univie.ac.at

Abstract

We evaluate and analyze the exact value of a measure for local genuine tripartite entanglement in the one-dimensional cluster-Ising model for spin-$\frac{1}{2}$ particles. This model is attractive since cluster states are considered to be relevant sources for applying quantum algorithms and the model is experimentally feasible. Whereas bipartite entanglement is identically vanishing, we find that genuine tripartite entanglement is non zero in the anti-ferromagnetic phase and also in the cluster phase well before the critical point. We prove that the measure of local genuine tripartite entanglement captures all the properties of the symmetry-protected topological quantum phase transition. Remarkably, we find that the amount of genuine tripartite entanglement is independent of whether the ground states satisfy or break the symmetries of the Hamiltonian. We provide also strong evidences that local genuine tripartite entanglement represents the unique non-vanishing genuine multipartite entanglement.

Keywords: quantum entanglement, scaling phenomena in complex systems, quantum phase transitions

Quantum many-body systems usually posses a highly entangled ground state that exhibits collective quantum phenomena. Therefore, the analysis of the entanglement properties of a ground state becomes an important resource that flanks the standard analysis based on the Grinzburg–Landau paradigm [1] that is based on spontaneous symmetry breaking and a non-

vanishing order parameter, e.g., 'magnetization' [2]. Although the presence and the importance of entanglement is recognized in many different physical contexts and physical systems, entanglement detection and quantification is a highly involved task (for mixed states). Except for the easiest case, bipartite spin-$\frac{1}{2}$ systems, no necessary and sufficient general method is known. The problem becomes much more pronounced for multipartite entanglement which has been found to play an essential role in many phenomena and may provide a high-capacity resource for quantum computing. Among multipartite entanglement *genuine* multipartite entanglement is the most interesting one since all subsystems truly contribute to the entanglement. For example, genuine multipartite entanglement is shown to be the necessary property for protecting a secret shared among many parties against eavesdropping or unfaithful parties [3].

In this letter we relate two rich phenomena in modern physics, i.e. the genuine multipartite entanglement and the quantum phase transition between a topological and an anti-ferromagnetic phase. Previous works have shown that quantum phase transitions can be characterized in terms of bipartite entanglement [4, 5] or in terms of the von Neumann entropy of bipartite spin–block entanglement [6–8], or via global geometric entanglement [9] or via analyzing the existence of values for which the entanglement is completely absent [10]. Recent works [11, 12] have shown the presence of genuine multipartite entanglement in subsystems of typical condensed matter systems by computing criteria capable of detecting different types of genuine multipartite entanglement.

This contribution shows, for the first time, that the exact amount of genuine tripartite entanglement can be computed exploiting a measure for genuine multipartite entanglement and that this measure can be used to characterize the quantum phase transition. In particular, our model exhibits a symmetry-protected topological phase; those phases are known to play a prominent role e.g. in the quantum Hall effect [13], for superconductivity [14], for the confinement problem in QCD or in string theory. The condensed matter model that we investigate has in one limit a pure Ising interaction and in the other limit a cluster state as a ground state. Cluster states are a special type of multi-qubit state of graph states which are conjectured to be important resources for quantum algorithms (see, e.g., [15]). This cluster-Ising model can be simulated, e.g., for cold atoms in a triangular optical lattice [16]. In the thermodynamic limit the anti-ferromagnetic phase is characterized by a standard staggered local order parameter whereas in the cluster phase one finds a gapped energy spectrum [17] with diverging localizable entanglement due to a non-vanishing string order parameter [18]. In summary, this system is interesting since it can be experimentally put to reality (e.g., via methods introduced in [19]), it is fully analytically solvable, has a quantum phase transition from an anti-ferromagnetic phase to a symmetry-protected topological phase [7, 20–22] and provides a physical platform for quantum computation [23].

We start our analysis by introducing the Hamiltonian and the definition of genuine multipartite entanglement. We find that the reduced density matrices of three adjacent spins obtained by ground states preserving all the symmetries of the Hamiltonian of the cluster-Ising model hold the property that they can be turned always in the *X*-form [24]. The *X*-form allows us to compute analytically the exact amount of the *genuine tripartite entanglement* [25, 26] which is in this case identical to the general criteria for detecting different types of multipartite entanglement introduced in [27]. We then prove that a non-vanishing value of such a measure of genuine tripartite entanglement characterizes as well the anti-ferromagnetic phase as the

cluster phase close to the quantum phase transition (except for the factorization point [10]). In particular, we prove that this measure captures all critical properties known as the universality property, i.e. the behavior at the critical point is independent of the finite size scaling. In a second step we extend our analysis to ground states breaking the Z_2-symmetry of the Hamiltonian in the anti-ferromagnetic phase. We find that even in this case the reduced density matrix posses the same value of genuine tripartite entanglement, i.e. symmetry breaking does not affect the amount of entanglement showing its generality. Last but not least we consider different subsets and analyze them according to their genuine multipartite entanglement content. Our results suggest that the genuine tripartite entanglement between three adjacent spins is the only source of genuine multipartite entanglement in this model.

To set the stage for our analysis let us introduce the one dimension cluster-Ising model, that is characterized by the interplay between a three-body cluster like interactions and a two-body anti-ferromagnetic Ising term

$$H = (-1 + \alpha) \sum_{i=-l}^{l} S_{i-1}^x S_i^z S_{i+1}^x + \alpha \sum_{i=-l-1}^{l} S_i^y S_{i+1}^y. \tag{1}$$

The number of spins in the chain are $N = 2l + 3$ and α is the relative weight between the two different interactions and may assume any values in the interval $[0, 1]$. S_i^μ are the standard spin-1/2 operators acting on the ith site. Note that all the evaluation made for finite size are done assuming open boundary conditions and N equal to an integer multiple of 3.

Regardless its apparent complexity the cluster-Ising model can be analytically solved making use of the Jordan–Wigner transformation that brings spin operators in fermionic ones [28]. With this transformation the spin model is mapped into a bilinear fermionic problem that can be analytically solved both for a finite size system and in thermodynamic limit (see appendix). Thanks to the existence of such analytical solutions, the phase diagram of the one dimensional cluster-Ising model in the thermodynamic limit can be computed [18, 22]. For $\alpha > \frac{1}{3}$ the system is in an anti-ferromagnetic phase characterized by a twofold degenerated ground state with a non vanishing staggered local order parameter along the y axis $m_y = (-1)^i \langle \sigma_i^y \rangle$. On the contrary when $\alpha < \frac{1}{3}$ the system is in the so called *cluster phase* with a four fold degenerate ground state that is characterized by a highly non local string order parameter.

The first remarkable result concerns the local entanglement properties in the cluster-Ising chain [22]. For any two spins taken out of the chain the entanglement is zero for all α (e.g., computed via Hill–Wootters concurrence [29] which is a necessary and sufficient measure of entanglement of bipartite spin-$\frac{1}{2}$ systems). Clearly, the vanishing of any pairwise entanglement disables the characterizing of the quantum phase transition or the critical properties of the complex system. This result and the fact that the residual tangle is fixed to its maximum value for ground states that satisfy the symmetry of the Hamiltonian and in the case of broken symmetry never drops to zero [22, 30] (except for $\alpha = 1$) suggest that genuine multipartite entanglement plays an important role in the cluster-Ising model.

Let us now define *genuine multipartite entanglement*. Let us consider a system consisting of n spin-$\frac{1}{2}$ particles. The state of this n spins is called k-separable if and only if it can be written in the form

$$\rho_{(k-\mathrm{sep})} = \sum_i p_i \left| \Psi^i_{(k-\mathrm{sep})} \right\rangle \left\langle \Psi^i_{(k-\mathrm{sep})} \right| \tag{2}$$

with $p_i \geqslant 0$ and $\sum_i p_i = 1$ and $|\Psi_{(k-\mathrm{sep})}\rangle = |\psi_1\rangle \otimes |\psi_2\rangle \otimes \ldots |\psi_k\rangle$, where $k \leqslant n$ and each ψ_i ($i = 1, \ldots k$) is living on different and non-overlapped subsets of spins. Note that biseparable states do not need to be separable via a specific partition since one sums up over different configurations. States which are not biseparable ($k = 2$) are dubbed genuine multipartite entangled. There is no closed formula that provides us with the value of the genuine multipartite entanglement in the general case. However, if density matrices can be turned in the so called X-matrix form [24]

$$\rho = \begin{pmatrix} t_1 & & & & & & & z_1 \\ & t_2 & & & & & z_2 & \\ & & \ddots & & & \iddots & & \\ & & & t_{n'} & z_{n'} & & & \\ & & & z_{n'}^* & s_{n'} & & & \\ & & \iddots & & & \ddots & & \\ & z_2^* & & & & & s_2 & \\ z_1^* & & & & & & & s_1 \end{pmatrix}, \tag{3}$$

in such a case it is possible to evaluate the genuine multipartite concurrence (C_{gm}) [25] that is a faithful measure of the genuine m-partite tangle ($m = 1 + \log_2 n'$). In the presence of a density matrix in X form the C_{gm} is given by [26]

$$C_{\mathrm{gm}} = 2 \max \left\{ 0, |z_i| - \sum_{j \neq i} \sqrt{s_j t_j} \right\}. \tag{4}$$

To begin, let us focus our analysis on the genuine tripartite entanglement and let us first consider the state ρ_3^T, a state obtained by projecting the thermal ground state that preserves all the symmetries of the Hamiltonian into the three central spins $\{-1, 0, 1\}$. We have

$$\begin{aligned} \rho_3^T = \frac{1}{8} \Big[& \mathbb{1} - a \left(\sigma_{-1}^y \sigma_0^y + \sigma_0^y \sigma_1^y \right) + a^2 \, \sigma_{-1}^y \sigma_1^y - b \, \sigma_{-1}^x \sigma_0^z \sigma_1^x \\ & + ba \left(\sigma_{-1}^x \sigma_0^x \sigma_1^z + \sigma_{-1}^z \sigma_0^x \sigma_1^x \right) + ba^2 \, \sigma_{-1}^z \sigma_0^z \sigma_1^z \Big], \end{aligned} \tag{5}$$

where $a = -G(1, \alpha) = \langle \sigma_0^y \sigma_1^y \rangle$, $b = G(-2, \alpha) = -\langle \sigma_{-1}^x \sigma_0^z \sigma_1^x \rangle$ and $G(n, \alpha)$ are the fermionic correlation functions (see appendix). In the case of a finite size system the fermionic correlation functions are evaluated numerically using an algorithm that generalizes the approach of [31]. On the contrary in the thermodynamic limit they are given by [22]

$$G(n, \alpha) = \frac{1}{\pi} \int_0^\pi \frac{\cos(n+2)x - \frac{2\alpha}{1-\alpha} \cos(n-1)x}{\Lambda(x, \alpha)} \mathrm{d}x, \tag{6}$$
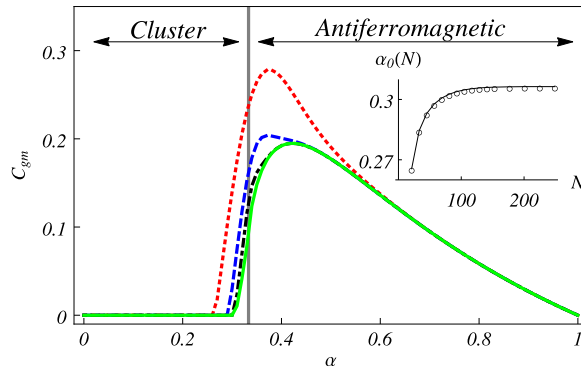
Figure 1. The genuine tripartite concurrence C_{gm} plotted for the three central spins in the chain as function of the parameter α for different lengths N of the spin chain. The different curves correspond to: red dotted line $N = 21$; blue dashed line $N = 45$; black dot-dashed line $N = 93$; green solid line $N = \infty$. The vertical grid line indicates the critical value $\alpha_c = 1/3$. In the inset we plot the behavior of $\alpha_0(N)$, i.e. the value α for which the measures become nonzero, as a function of the the length of the chain.

where

$$\Lambda(x, \alpha) = \left[1 + \left(\frac{2\alpha}{1 - \alpha} \right)^2 - \frac{4\alpha}{1 - \alpha} \cos(3x) \right]^{\frac{1}{2}}. \tag{7}$$

Regardless of the value of the fermionic correlation functions, applying the unitary operator

$$U = e^{-i\frac{\pi}{4}\sigma^x_{-1}} \otimes e^{-i\frac{\pi}{4}\sigma^x_0} \otimes e^{-i\frac{\pi}{4}\sigma^x_1} \tag{8}$$

turns ρ_3^T into the X-form with the additional symmetry that $t_i = s_i$ with $i = 1,...,4$ (corresponding to the vanishing of $\langle \sigma_i^\gamma \rangle = 0 \; \forall \gamma = x, y, z$). From equation (5) it is straightforward to obtain the value of the genuine tripartite entanglement as

$$C_{gm} = \frac{1}{4} \max \left\{ 0, (1 + a)^2(1 + b) - 4 \right\}, \tag{9}$$

whose behavior as a function of α is plotted both in thermodynamic limit and for finite size systems in figure 1. Independently, of the number of spins N the behavior of the measure C_{gm} is similar and converges with increasing number fast to a nonzero value in the anti-ferromagnetic phase (except the factorization point $\alpha = 1$). Remarkably, it becomes nonzero already well before the critical point $\alpha_c = \frac{1}{3}$ and also independently of N. In the inset of figure 1 we have plotted the dependence of the value of α when it becomes nonzero in dependence of N. For the thermodynamic limit we obtain $\alpha_0(\infty) \simeq 0.3064$, a value clearly below $\alpha_c = 1/3$. This rising of the genuine tripartite measure before the quantum phase transition plays the roles of a precursor of the quantum phase transition.

We can go one step further by considering the derivative $\partial_\alpha C_{gm} = \partial C_{gm}/\partial \alpha$ and exploring its non-trivial behavior close to the quantum critical point. For the finite size case we find a maximum before the critical point that converges with increasing number of sizes N to a maximum at the critical point (see inset of figure 2). Being more precise the maximum value of $\partial_\alpha C_{gm}$ diverges logarithmically with N as
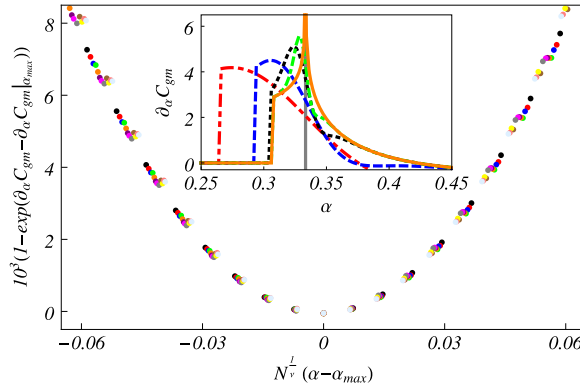
Figure 2. The universality (i.e., the fact that critical properties depend only on the size of the system and the broken symmetry in the ordered phase) of the (rescaled) genuine multipartite entanglement is checked by plotting the finite-size scaling with respect to C_{gm}, according to the procedure described in [2]. The different colors represent different data that goes from 45 to 249 spins. The critical exponent is taken equal to $\nu = 1$. In the inset we plot the behavior of $\partial_\alpha C_{\mathrm{gm}}$ close to α_c for chains of different lengths as function of α: red dot-dot-dashed line $N = 21$; blue dashed line $N = 45$; black dotted line $N = 129$; green dot-dashed line $N = 249$, orange solid line $N = \infty$.

$$\partial_\alpha C_{\mathrm{gm}}\Big|_{\alpha=\alpha_{\max}} = 0.24(1)\log N + \mathrm{const}, \tag{10}$$

and in the thermodynamic limit the derivative $\partial_\alpha C_{\mathrm{gm}}$ diverges approaching the critical value $\alpha = \alpha_c \equiv \frac{1}{3}$

$$\lim_{N\longrightarrow\infty} \partial_\alpha C_{\mathrm{gm}} = 0.240(1)\big(-\log|\alpha - \alpha_c|\big) + \mathrm{const}. \tag{11}$$

According to the scaling ansatz [2, 4, 11], whose validity is shown in figure 2, in the case of logarithmic singularities, the ratio between the two prefactors of the logarithm in equation (10) and (11) is the exponent ν that governs the divergence of the correlation length $\xi \approx |\alpha - \alpha_c|^{-\nu}$. We find $\nu = 1$ that is consistent with the characterization obtained from the analysis of the behavior of the correlation function.

In the cluster phase, regardless the four-fold degeneracy of the ground space, there is no ground state that breaks the symmetry of the Hamiltonian, in contrast to the anti-ferromagnetic phase. Let us superpose two ground states that each preserves in the anti-ferromagnetic phase all the symmetries of the Hamiltonian, then we obtain a maximally symmetry broken ground state which reduced density matrix of three adjacent spins is given by

$$\rho_3^B = \rho_3^T + \frac{1}{8}\Big[c\left(\sigma_{-1}^y - \sigma_0^y + \sigma_1^y\right) - d\,\sigma_{-1}^y\sigma_0^y\sigma_1^y \Big], \tag{12}$$

where c and d are the expectation values of $\langle\sigma_i^y\rangle_B$ and $\langle\sigma_{i-1}^y\sigma_i^y\sigma_{i+1}^y\rangle_B$, respectively. The subscript B indicates that the average is evaluated on states breaking maximally the symmetry. Since the additional terms are only proportional to σ^y the X-form can be recovered using the same local unitary transformation as defined in equation (8). Moreover, as shown in the appendix, $c = d$ holds and, consequently, the same value of the genuine tripartite measure is obtained. This also holds for any ground state that breaks the Z_2 symmetry. Hence, we conclude that C_{gm}, differently from what happens for the pairwise entanglement between two spins, e.g., in the *XY*
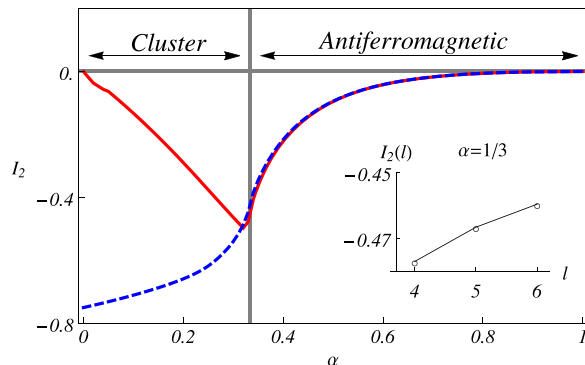
Figure 3. The function I_2 (optimized over all possible $\Phi_{1,2}$) detecting genuine multipartite entanglement [27] if greater than zero is plotted as function of α for the subsets of three spins $\{-2, 0, 1\}$ (blue dashed lines) and the subsets of four spins $\{-2, -1, 0, 1\}$ (red solid lines). The inset shows I_2 for $l = 4, 5, 6$ adjacent spins for $\alpha = \frac{1}{3}$. No genuine multipartite entanglement is detected.

model [32], does not depend on the choice of the ground state and, therefore, captures all the relevant properties of the system.

Let us now investigate the entanglement properties of different subsets. Increasing the distance between the spins but still preserving the symmetry of the subset, i.e. considering the subset $\{-s, 0, s\}$ we find that the reduced density matrices can be brought into the X-form but the measure vanishes. If we increase the subset, e.g., consider the subset of four spins $\{-2, -1, 0, 1\}$ we find that the reduced density matrix can no longer be brought into the X-form. This is due to the presence of non-vanishing two body correlation function along the x direction $\langle \sigma_i^x \sigma_j^x \rangle$.

Therefore, to study the presence of genuine multipartite entanglement we use the approach introduced in [27]. At the heart of this approach are convex functions of the density matrix ρ and permutations operators $\mathcal{P}$ on subsets β defined on copies of ρ which are symmetries of a certain type of multipartite entanglement, i.e. $[\mathcal{P}_\beta, \rho^{\otimes 2}] = 0 \implies \rho^{\otimes 2} = \mathcal{P}_\beta \rho^{\otimes 2} \mathcal{P}_\beta$. If the symmetry is satisfied the following convex function is bounded by

$$I_k := \left| \langle \Phi_1 | \rho | \Phi_2 \rangle \right| - \sum_{\{\beta\}} \left(\prod_{j=1}^k \left\langle \Phi_1 \Phi_2 \left| P_{\beta,j}^\dagger \rho^{\otimes 2} P_{\beta,j} \right| \Phi_1 \Phi_2 \right\rangle \right)^{\frac{1}{2k}} \leqslant 0 \qquad (13)$$

for any arbitrary states $\Phi_{1,2}$ with dimension of ρ and j denotes a certain partition in the subset β and k defines the number of partitions one is interested in. The states satisfying the above inequality for a given partition k are just the k-separable states defined in equation (2), hence, any positive values detect states that are not k-separable. In figure 3 we plotted, for each α the maximum value over all possible choices of $\Phi_{1,2}$. No genuine multipartite entanglement is detected for any value of α, moreover, the value is rather far away from the bound zero. In the inset of figure 3 we plotted the value of I_2 at the critical point for four to six adjacent spins. We observe only a very small increase of the value. These results strongly suggest that there is no other type of genuine multipartite entanglement present than the genuine tripartite one of three adjacent spins. This fact, together with the absence of bipartite entanglement between a couple of spins regardless the distance and the Hamiltonian parameter α is completely unexpected. It seems to suggest that the ground state is organized in trimers, or, in other words, it suggests the

presence of a sub-leading order similar to and even stronger than the one discovered in the *XY* model below the factorization point [33].

    Summarizing, in the present letter we have provided the first evaluation of the genuine multipartite entanglement for the plethora of ground states of a condensed matter system for which bipartite entanglement is zero. We have determined analytically the amount of genuine tripartite entanglement for a subset consisting of three spins for finite size systems and in the thermodynamic limit. We find for any size of the system that local genuine tripartite entanglement is nonzero before the critical point $\alpha = \frac{1}{3}$, i.e. genuine tripartite entanglement acts as a precursor of the quantum phase transition. Moreover, we have proven that the non-trivial behavior of the genuine tripartite entanglement measure characterizes the critical and scaling properties of the quantum phase transition fully. The existence of these non-trivial quantum correlations at any size around the critical point and the independence on the chosen ground states is very different to other condensed matter systems, e.g. the *XY* model. We have further provided strong evidence that the genuine tripartite entanglement is the only manifestation of genuine multipartite entanglement in this particular condensed matter system.

    In future, it would be desirable to extend such analysis to other condensed matter systems and to try to connect the presence of genuine multipartite entanglement both with the behavior of the entanglement spectrum [33] and with scaling properties of the quantum frustration [34].

Acknowledgements

Appendix

In this section we describe how the Hamiltonian is diagonalized, subsequently how one obtains the fermionic correlation functions and from them the spin correlations functions that are analyzed in the main manuscript.

A.1. Diagonalization of the Hamiltonian

Despite the presence of three-body interactions the Hamiltonian (1) can be mapped into a delocalized fermionic form via a generalization of the approach described in [31]. To obtain this map we introduce the Jordan–Wigner transformation [28] that connects the spin operators to the fermionic operator via

$$c_j = \left(\overset{j-1}{\underset{i=-l-1}{\bigotimes}} 2S_i^z \right) S_j^- , \quad c_j^\dagger = \left(\overset{j-1}{\underset{i=-l-1}{\bigotimes}} 2S_i^z \right) S_j^+, \tag{A.1}$$

where $S_i^{\pm} = S_i^x \pm iS_i^y$. Applying this transformation to the Hamiltonian (1) we obtain

$$
\begin{aligned}
H = \ & \frac{1-\alpha}{8} \sum_{i=-l}^{l} \left(c_{i-1}^{\dagger} c_{i+1}^{\dagger} + c_{i-1}^{\dagger} c_{i+1} + \text{h.c.} \right) \\
& + \frac{\alpha}{4} \sum_{i=-l-1}^{l} \left(c_i^{\dagger} c_{i+1}^{\dagger} + c_i^{\dagger} c_{i+1} + \text{h.c.} \right)
\end{aligned}
\tag{A.2}
$$

This Hamiltonian corresponds to a so-called free fermion case in which non-interacting fermions can jump between nearest and next to nearest neighbours of the chain via open boundary conditions, i.e. $N = 2l + 3$. This Hamiltonian can be brought in a diagonal form

$$
H = \sum_k \lambda_k \, \eta_k^{\dagger} \eta_k + \text{const.}
\tag{A.3}
$$

using the following linear transformation

$$
\begin{aligned}
\eta_k = \ & \sum_{i=-l-1}^{l+1} \frac{\phi_{k,i} + \psi_{k,i}}{2} c_i + \frac{\phi_{k,i} - \psi_{k,i}}{2} c_i^{\dagger} \\
\eta_k^{\dagger} = \ & \sum_{i=-l-1}^{l+1} \frac{\phi_{k,i} + \psi_{k,i}}{2} c_i^{\dagger} + \frac{\phi_{k,i} - \psi_{k,i}}{2} c_i,
\end{aligned}
\tag{A.4}
$$

where both vectors ϕ_k and ψ_k are a set of N vectors with N components that are solutions of the coupled equations

$$
\begin{aligned}
\lambda_k \psi_k = \ & \phi_k (\mathbf{A} + \mathbf{B}) \\
\lambda_k \phi_k = \ & \psi_k (\mathbf{A} - \mathbf{B}).
\end{aligned}
\tag{A.5}
$$

Here the matrix $\mathbf{A}$ (symmetric) and $\mathbf{B}$ (anti-symmetric) are, respectively,

$$
\mathbf{A} = \frac{1}{8}
\begin{pmatrix}
0 & 2\alpha & \gamma & 0 & 0 & 0 & 0 & 0 & 0 & 0 \\
2\alpha & 0 & 2\alpha & \gamma & 0 & 0 & 0 & 0 & 0 & 0 \\
\gamma & 2\alpha & 0 & 2\alpha & \gamma & 0 & 0 & 0 & 0 & 0 \\
& \ddots & \ddots & \ddots & \ddots & \ddots & & & & \\
& & \ddots & \ddots & \ddots & \ddots & \ddots & & & \\
& & & \ddots & \ddots & \ddots & \ddots & \ddots & & \\
& & & & \ddots & \ddots & \ddots & \ddots & \ddots & \\
0 & 0 & 0 & 0 & 0 & \gamma & 2\alpha & 0 & 2\alpha & \gamma \\
0 & 0 & 0 & 0 & 0 & 0 & \gamma & 2\alpha & 0 & 2\alpha \\
0 & 0 & 0 & 0 & 0 & 0 & 0 & \gamma & 2\alpha & 0
\end{pmatrix}
\tag{A.6}
$$

and

$$\mathbf{B} = \frac{1}{8} \begin{pmatrix} 0 & 2\alpha & \gamma & 0 & 0 & 0 & 0 & 0 & 0 & 0 \\ -2\alpha & 0 & 2\alpha & \gamma & 0 & 0 & 0 & 0 & 0 & 0 \\ -\gamma & -2\alpha & 0 & 2\alpha & \gamma & 0 & 0 & 0 & 0 & 0 \\ & \ddots & \ddots & \ddots & \ddots & \ddots & & & & \\ & & \ddots & \ddots & \ddots & \ddots & \ddots & & & \\ & & & \ddots & \ddots & \ddots & \ddots & \ddots & & \\ & & & & \ddots & \ddots & \ddots & \ddots & \ddots & \\ 0 & 0 & 0 & 0 & 0 & -\gamma & -2\alpha & 0 & 2\alpha & \gamma \\ 0 & 0 & 0 & 0 & 0 & 0 & -\gamma & -2\alpha & 0 & 2\alpha \\ 0 & 0 & 0 & 0 & 0 & 0 & 0 & -\gamma & -2\alpha & 0 \end{pmatrix} \tag{A.7}$$

and $\gamma = 1 - \alpha$. Either ψ_k or ϕ_k can be eliminated from the equations (A.5) resulting in

$$\lambda_k^2 \psi_k = \psi_k (\mathbf{A} + \mathbf{B})(\mathbf{A} - \mathbf{B})$$
$$\lambda_k^2 \phi_k = \phi_k (\mathbf{A} - \mathbf{B})(\mathbf{A} + \mathbf{B}). \tag{A.8}$$

For $\lambda_k \neq 0$ we can choose one of these two equations that gives us one set of vectors and with the help of the equations (A.5) one obtains the second set of vectors. For $\lambda_k = 0$ one obtains ψ_k and ϕ_k from the equations (A.5).

A.2. Fermionic correlation functions

The set of vectors ψ_k and ϕ_k plays an important role for the evaluation of the fermionic correlations functions. To see that let us introduce two new fermionic operators

$$\nu_i = c_i^\dagger + c_i; \qquad \mu_i = c_i^\dagger - c_i. \tag{A.9}$$

The advantage of using this set of operators, μ_i and ν_i, with respect to the set of operators c_i and $c_i^\dagger$ comes from the fact that, taking into account the equation (A.4), we obtain particular simplifications computing the expectation values of the product of two operators, in particular

$$\left\langle \mu_i \mu_k \right\rangle = \sum_l \phi_{l,i} \phi_{l,j} = \delta_{ik}$$
$$\left\langle \nu_i \nu_k \right\rangle = -\sum_l \psi_{l,i} \psi_{l,j} = -\delta_{ik}$$
$$\left\langle \nu_i \mu_k \right\rangle = -\left\langle \mu_i \nu_k \right\rangle = -\sum_l \psi_{l,i} \phi_{l,j} = G_{i,j}(\alpha). \tag{A.10}$$

In the finite size case the $G_{i,j}(\alpha)$ depends on the choice of the site i and j and, therefore, also the spin correlation functions depend on the position of the spins in the chain. However, if we evaluate the correlation functions between three central spins of a chain with an odd N, the mirror symmetry plays the role of the invariance under spatial translation, imposing that

$$\left\langle S_{-1}^\alpha S_0^\beta \right\rangle = \left\langle S_1^\alpha S_0^\beta \right\rangle \qquad \forall \ \alpha, \beta = x, y, z. \tag{A.11}$$

On the contrary, in the thermodynamic limit the invariance under spatial translation is restored by the fact that the end of the chain is infinitely far away. In this case, imposing the invariance under spatial translation, we can solve equation (A.5) considering that each

component of ϕ_k and ψ_k vectors obeys to the following rule

$$\phi_{k,l} = \frac{q_{k,l}}{\sqrt{N}} e^{-i\frac{2\pi}{N}kl} ; \qquad \psi_{k,l} = \frac{q'_{k,l}}{\sqrt{N}} e^{-i\frac{2\pi}{N}kl}. \tag{A.12}$$

With a long but straightforward evaluation we obtain the fermionic correlation functions in the thermodynamic limit given in equations (6) and (7), respectively.

A.3. Spin correlation functions

Having introduced a method to evaluate the fermionic correlation functions we can compute the spin correlation functions from which we obtain any reduced density matrix. We can divide the spin correlation functions in two families. The first consists of correlation functions from operators that do not break the symmetry of the Hamiltonian. In this case transforming the spin operators into the fermionic operators μ_i and ν_i one always obtains an operator constructed via an equal number of μ_i and ν_i. Applying the Wick's theorem we then obtain the expression of the correlation functions in terms of the $G(n, \alpha)$. Let us also point out that the dependence of the spin correlation functions on the fermionic correlation functions are independent of the model. A list of these spin correlation functions given in terms of fermionic correlation functions can be founded in [12].

The situation is much more involved in the case the symmetry of the Hamiltonian is broken. In this second case, if we try to apply the same strategy as described above, we immediately observe that the elements due to parity immediately vanish. In fact, re-writing the operators in terms of μ_i and ν_i, we obtain an expression with different numbers of fermionic operators, each one referring to distinct sites, and, in agreement with equation (A.10), this implies that the correlation function must be zero. This result holds for all ground states that preserve the symmetry of the Hamiltonian, however, in the thermodynamic limit and in the anti-ferromagnetic phase one has also ground states that break the Z_2 symmetry of the Hamiltonian. For these ground states some of these correlation functions are expected to be different from zero.

To evaluate these correlation functions we adopt the approach of Barouch and McCoy [35]. Given an operator $O_{\{k\}}$ defined on a set of spins $\{k\}$ that does not commute with the parity operator along the Z axis one can define the correlation function $\langle O_{\{k\}} \rangle_B$ via

$$\left\langle O_{\{k\}} \right\rangle_B = \lim_{r \to \infty} \sqrt{\left\langle O_{\{k\}} O_{\{k\}+r} \right\rangle}. \tag{A.13}$$

For analyzing the entanglement properties of three adjacent spins one has to compute all the one, two and three body correlation functions that do not commute with the parity operators along the Z axis. All the correlation functions of this type are vanishing in the limit of $r \to \infty$ except $\langle \sigma_i^y \rangle_B$ and $\langle \sigma_{i-1}^y \sigma_i^y \sigma_{i+1}^y \rangle_B$. In figure A1 we have reported, for some values of α, the values of $\langle \sigma_i^y \rangle_B$ and $\langle \sigma_{i-1}^y \sigma_i^y \sigma_{i+1}^y \rangle_B$. We observe that the further we are away from the quantum critical point the faster is the convergence of the correlation functions to the asymptotic values. Moreover, for all α we observe that $\langle \sigma_i^y \rangle_B = \langle \sigma_{i-1}^y \sigma_i^y \sigma_{i+1}^y \rangle_B$ for large enough r (we have tested this relation for more that 1000 different values of $\alpha > \alpha_c$). The fact that this equality holds imposes that the genuine tripartite entanglement between three adjacent spins does not depend on the particular ground state selected as emphasized in the main body of the manuscript.
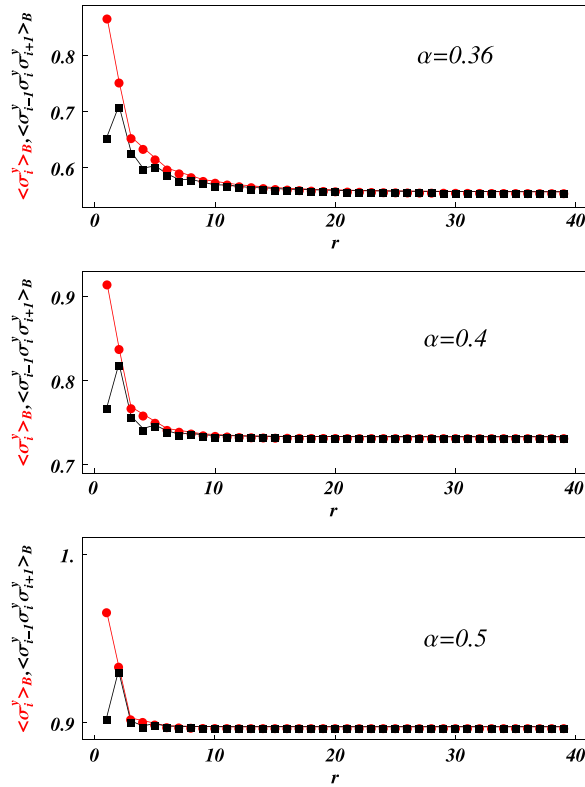
Figure A1. The figures show the values of $\langle \sigma_i^y \rangle_B$ (red points) and $\langle \sigma_{i-1}^y \sigma_i^y \sigma_{i+1}^y \rangle_B$ (black squares) for different distances r and for different values of α in the anti-ferromagnetic phase.

References

[1] Amico L, Fazio R, Osterloh A and Vedral V 2008 *Rev. Mod. Phys.* **80** 517

[2] Barber M N 1983 *Phase Transitions and Critical Phenomena* vol 8 ed C Domb and J L Leibovitz (London: Academic) p 146

[3] Schauer S, Huber M and Hiesmayr B C 2010 *Phys. Rev.* A **82** 062311

[4] Osterloh A, Amico L, Falci G and Fazio R 2002 *Nature* **416** 608

[5] Osborne T J and Nielsen M A 2002 *Phys. Rev.* A **66** 032110

[6] Holzhey C, Larsen F and Wilczek F 1994 *Nucl. Phys.* B **424** 443
Vidal G, Latorre J I, Rico E and Kitaev A 2003 *Phys. Rev. Lett.* **90** 227902
Latorre J I, Rico E and Vidal G 2004 *Quantum Inf. Comput.* **4** 48
Calabrese P and Cardy J 2004 *J. Stat. Mech.* P06002

[7] Chen X, Gu Z-C and Wen X-G 2010 *Phys Rev.* B **82** 155138

[8] Jiang H-C, Wang Z and Balents L 2012 *Nat. Phys.* **8** 902

[9] Wei T-C, Das D, Mukhopadyay S, Vishveshwara S and Goldbart P M 2005 *Phys. Rev.* A **71** 060305(R)

[10] Giampaolo S M, Adesso G and Illuminati F 2008 *Phys. Rev. Lett.* **100** 197201
Giampaolo S M, Adesso G and Illuminati F 2009 *Phys. Rev.* B **79** 224434
Giampaolo S M, Adesso G and Illuminati F 2010 *Phys. Rev. Lett.* **104** 207202

[11] Giampaolo S M and Hiesmayr B C 2013 *Phys. Rev.* A **88** 052305

[12] Hofmann M, Osterloh A and Gühne O 2014 *Phys. Rev.* B **89** 134101

[13] Kane C L and Mele E J 2005 *Phys. Rev. Lett* **95** 146802

[14] Volovik G E 2003 *The Universe in a Helium Droplet* (Oxford: Clarendon)

[15] Bruss D and Macchiavello C 2011 *Phys. Rev.* A **83** 052313

[16] Pachos J K and Plenio M B 2004 *Phys. Rev. Lett.* **93** 056402

    Becker C, Soltan-Panahi P, Kronjäger J, Dörscher S, Bongs K and Sengstock K 2010 *New J. Phys.* **12** 065025

[17] Popp M, Verstraete F, Martín-Delgado M A and Cirac J I 2005 *Phys. Rev.* A **71** 042306

[18] Venuti L C and Roncaglia M 2005 *Phys. Rev. Lett.* **94** 207207

[19] Gabriel A and Hiesmayr B C 2013 *Europhys. Lett.* **101** 30003

    Spengler C, Huber M, Brierley S, Adaktylos T and Hiesmayr B C 2012 *Phys. Rev.* A **86** 022311

[20] Kou S-P and Wen X-G 2009 *Phys. Rev.* B **80** 224406

[21] Son W, Amico L, Fazio R, Hamma A, Pascazio S and Vedral V 2011 *Europhys. Lett.* **95** 50001

[22] Smacchia P, Amico L, Facchi P, Fazio R, Florio G, Pascazio S and Vedral V 2011 *Phys. Rev.* A **84** 022304

[23] Briegel H J and Raussendorf R 2001 *Phys. Rev. Lett.* **86** 910

    Miyake A 2010 *Phys. Rev. Lett.* **105** 040501

    Renes J M, Miyake A, Brennen G K and Bartlett S D 2013 *New J. Phys.* **15** 025020

    Wu J-Y, Rossi M, Kampermann H, Severini S, Chuan Kwek L, Macchiavello C and Bruss D 2014 *Phys. Rev.* A **89** 052335

[24] Yu T and Eberly J H 2007 *Quantum Inf. Comput.* **7** 459

[25] Hiesmayr B C and Huber M 2008 *Phys. Rev.* A **78** 012342

    Ma Z-H, Chen Z-H, Chen J-L, Spengler Ch, Gabriel A and Huber M 2011 *Phys. Rev.* A **83** 062325

[26] Hashemi Rafsanjani S M, Huber M, Broadbent C J and Eberly J H 2012 *Phys. Rev.* A **86** 062303

[27] Huber M, Mintert F, Gabriel A and Hiesmayr B C 2010 *Phys. Rev. Lett.* **104** 210501

    Gabriel A, Hiesmayr B C and Huber M 2010 *Quantum Inf. Comput.* **10** 829

[28] Jordan P and Wigner E 1928 *Z. Phys.* **47** 631

[29] Hill S and Wootters W K 1997 *Phys. Rev. Lett.* **78** 5022

    Wootters W K 1998 *Phys. Rev. Lett.* **80** 2245

[30] Coffman V, Kundu J and Wootters W K 2000 *Phys. Rev.* A **61** 052306

    Osborne T J and Verstraete F 2006 *Phys. Rev. Lett.* **96** 220503

[31] Lieb E, Schultz T and Mattis D 1961 *Ann. Phys.* **16** 407

[32] Osterloh A, Palacios G and Montangero S 2006 *Phys. Rev. Lett.* **97** 257201

[33] Giampaolo S M, Montangero S, Dell'Anno F, de Siena S and Illuminati F 2013 *Phys. Rev.* B **88** 125142

[34] Giampaolo S M, Gualdi G, Monras A and Illuminati F 2011 *Phys. Rev. Lett.* **107** 260602

    Marzolino U, Giampaolo S M and Illuminati F 2013 *Phys. Rev.* A **88** 020301(R)

[35] Barouch E and McCoy B 1971 *Phys. Rev.* A **3** 786